Drawing of Self-Reinforced Cellulose Films

Wolfgang Gindl,[1] Jozef Keckes[2]

[1]*Department of Materials Science and Process Engineering, University of Natural Resources and Applied Life Sciences, Vienna, Austria*
[2]*Erich Schmid Institute of Materials Science, Austrian Academy of Sciences and Institute of Metal Physics, University of Leoben, Leoben, Austria*

Received 16 May 2006; accepted 28 August 2006
DOI 10.1002/app.25434
Published online in Wiley InterScience (www.interscience.wiley.com).

ABSTRACT: Self-reinforced cellulose films were prepared by incomplete dissolution of commercial microcrystalline cellulose in LiCl/DMAc solvent and subsequent coagulation of regenerated cellulose in the presence of undissolved microcrystalline cellulose. By drawing in wet conditions and subsequent drying, preferred orientation was introduced into the self-reinforced cellulose films, resulting in significantly improved tensile strength of up to 430 MPa and modulus of elasticity of up to 33 GPa. A linear relationship was observed between applied draw, and the orientation of cellulose in the films, and the measured elastic modulus and tensile strength, respectively. The optically transparent drawn films significantly surpass the strength and modulus of elasticity of current all-bio-based planar materials and may therefore present a bio-degradable alternative to nonbio-based materials with similar performance. © 2006 Wiley Periodicals, Inc. J Appl Polym Sci 103: 2703–2708, 2007

Key words: cellulose; composites; drawing; mechanical properties; orientation

INTRODUCTION

''Green'' composites consisting of reinforced bio-based polymers[1] are subject to intense interest with regard to the development of sustainable and renewable materials for the future.[2,3] Important reinforcement options for such polymers are montmorillonite clay[4] and cellulosic fibers of natural and man-made origin.[5–7] With a chain modulus of elasticity of 138 GPa[8] and an estimated tensile strength of several GPa,[9] the reinforcement potential of natural cellulose, which is present in the crystalline conformation of cellulose I, is high in theory. In practice, the high reinforcement potential of natural cellulose fibers is only realized in combinations of cellulose nanofibrils with nonbio-based matrix polymers.[10,11] Recently it was shown that this limitation can be overcome by making use of the principle of self-reinforcement of cellulose films.[12,13] This technique consists of the interruption of dissolution of cellulose I at a certain stage in the production of regenerated cellulose. Thus, a significant amount of cellulose I remains undissolved upon coagulation of the dissolved cellulose, resulting in a regenerated cellulose film reinforced by cellulose I. Regenerated cellulose is usually obtained by dissolution of natural cellulose (cellulose I) in a suitable solvent and subsequent coagulation. The main industrial use of this process is in the spinning of rayon and lyocell fibers, and in the production of cellophane films. By contrast to natural cellulose, regenerated cellulose is present in the crystalline conformation of cellulose II. The modulus of elasticity of cellulose II is 88 GPa[8] and its theoretical tensile strength is 3.7 GPa.[14] When spun into fibers, a maximum tensile strength of 1.8 GPa and a modulus of elasticity of up to 55 GPa were observed for regenerated cellulose.[14] By comparison, the properties of cellophane films are typically 5.4 GPa for the modulus of elasticity and 125 MPa for tensile strength, and up to 8 GPa and 300 MPa, respectively, for melt-blown cellulose films from NMMO-solution (lyocell process), depending on the degree of preferred orientation.[15] Self-reinforced cellulose films profit from the higher stiffness and strength of cellulose I nanocrystals compared to cellulose II. It was shown that, by varying the ratio of cellulose I/cellulose II, the tensile strength, and modulus of elasticity of self-reinforced cellulose films can be tuned.[13]

The mechanical properties of polymers can be greatly changed by drawing. Drawing of polymer fibers and films is performed during the consolidation from the liquid to the solid state, or in solid state below the glass transition temperature (cold drawing) or at elevated temperature.[16–20] Due to drawing, the molecular chains in a polymer gradually align with the direction of applied strain, which in turn introduces mechanical anisotropy. In the present article we

Correspondence to: W. Gindl (wolfgang.gindl@boku.ac.at).

Journal of Applied Polymer Science, Vol. 103, 2703–2708 (2007)

demonstrate how the mechanical properties of self-reinforced cellulose films change by introducing preferred orientation through drawing in wet condition and subsequent drying.

MATERIALS AND METHODS

Films of self-reinforced regenerated cellulose obtained by incomplete dissolution of commercial microcrystalline cellulose (Aldrich 31,069-7, MCC) in a solution of lithium chloride (LiCl) in *N*-dimethylacetamide (DMAc) were prepared as described by Gindl and Keckes.[13] Briefly, 2 g MCC was dehydrated in methanol and in DMAc. In parallel, 8 g LiCl were dissolved in 100 mL DMAc. After decanting DMAc from the dehydrated MCC, the LiCl/DMAc solution was added to the cellulose and stirred for 5 min. Subsequently, the solution was poured into a 250 mm diameter Petri dish and left in a hood for 12 h. During this time, the solution coagulated to a transparent, 4 mm thick gel-like film due to uptake of moisture from the ambient air. Thereafter, the films were washed repeatedly in distilled water to remove solvent, and dried between gently compressed sheets of paper. The air-dry films of self-reinforced cellulose (thickness = 0.2 mm) obtained by this procedure were immersed in distilled water for 5 min and subsequently cut into strips of 50 mm length and 5 mm width. The wet, water-swollen strips were mounted in a Zwick 20 kN tensile testing machine and stretched to draw ratios (D_R, the ratio between specimen length after stretching and before stretching) of 1.1, 1.25, and 1.5 at a speed of 10 mm min^{-1} at ambient temperature (20°C). Stretching experiments at elevated temperature (90°C) were also performed but failed due to premature fracture of the specimens. Similarly, draw ratios > 1.5 could not be obtained due to fracture of the strained films. In stretched condition, the strips were dried by hot air and subsequently released from the testing machine. No noticeable shrinkage occurred upon specimen removal from the testing machine. Thereafter, the drawn specimens were left to equilibrate to ambient conditions (20°C, 60% rel. humidity) overnight. For mechanical testing, the specimens were again fixed to a tensile testing machine and tested at a speed of 1 mm min^{-1}. Drawn samples not tested in tensile testing were characterized by wide angle x-ray scattering using a *Nanostar* (Bruker AXS) system with a beam diameter of 100 μm and a two dimensional (2D) wire detector (Hi-Star). By radial integration of the intensity of 2D detector images, 2θ profiles were obtained. From these profiles, crystallinity (x_c) was determined from the ratio of crystalline scattering versus total scattering, whereby the amorphous contribution was estimated from an amorphous standard obtained by ball milling. From the 2θ profiles, the ratio of cellulose I/cellulose II was roughly estimated by comparing the respective peak height as described by Gindl and Keckes.[13] To quantify the degree of the preferred orientation in the drawn cellulose films, the orientation factor $\langle \cos^2 \phi \rangle$ of the *c* crystallographic axis of cellulose was evaluated from WAXS 2D detector images.[21] The azimuthal intensity distribution along the combined cellulose I (200) and cellulose II (110/020) Debey-Scherrer ring was obtained by integrating the 2D frames using Fit2D software (http://www.esrf.fr/computing/scientific/FIT2D/). The integrated intensity data was then used to calculate the orientation factors numerically for each WAXS pattern according to

$$\langle \cos^2 \phi \rangle = \frac{\int_0^{\pi/2} I(\phi) \cos^2 \phi \sin \phi d\phi}{\int_0^{\pi/2} I(\phi) \sin \phi d\phi} \quad (1)$$

where φ represents the azimuthal angle and I(φ) is the intensity along the Debey-Scherrer ring. Subsequently, the more commonly used orientation factor f_c was calculated from $\langle \cos^2 \phi \rangle$ according to

$$f_c = \frac{3(\cos^2 \phi) - 1}{2} \quad (2)$$

Maximum orientation parallel to the reference direction is found when $f_c = 1$, whereas $f_c = 0$ indicates random orientation.[21] Finally, the average orientation of both amorphous and crystalline cellulose was characterized by means of birefringence measurements with a Zeiss Axioimager microscope equipped with a Berek compensator 5λ. The specimen birefringence Δn was obtained by dividing the measured retardation of polarized light by the thickness of the cellulose film. Herman's orientation factor, which describes the average orientation of both the crystalline and amorphous phases, may be obtained by dividing the measured birefringence Δn by the maximum birefringence Δn_{max} for cellulose. A value of 0.081 for Δn_{max} was recently proposed by Kong and Eichhorn.[22]

RESULTS AND DISCUSSION

A sample of self-reinforced cellulose film used in the present study is shown in Figure 1. The film is optically transparent, as demonstrated by the good visibility of the underlying sheet of printed paper. From 2θ profiles (Fig. 2) obtained by radial integration of WAXS 2D detector images, a crystallinity of 46% was calculated. The 2θ profile of the self-reinforced cellulose film shown in Figure 2 is very similar to

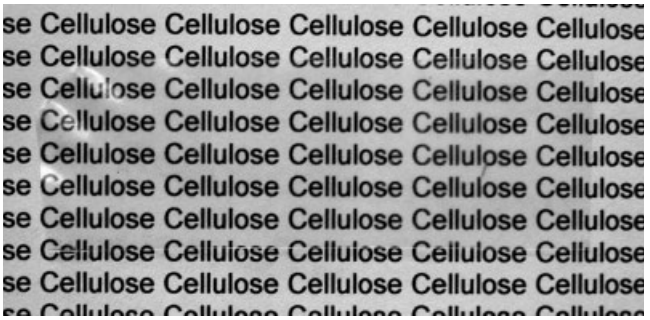

Figure 1 Photograph of a self-reinforced cellulose film placed on a sheet of paper demonstrating excellent transparency.

regenerated cellulose at first view. However, different crystallinity is apparent, and a distinct shoulder at the scattering angle of the most intense cellulose I reflection (200 reflection at $2\theta \sim 22.6^\circ$) indicates the presence of cellulose I crystallites. The crystalline fraction of the self-reinforced film contains estimated 25% cellulose I and 75% cellulose II (estimation based on peak height ratio as described in Ref. 13). To introduce preferred orientation into the self-reinforced cellulose film, it was drawn to various extents. Before drawing, dried self-reinforced films were immersed in water for swelling, since the adsorption of water to accessible cellulose hydroxyl groups increases chain mobility by weakening of intramolecular[23] and intermolecular hydrogen bonds,

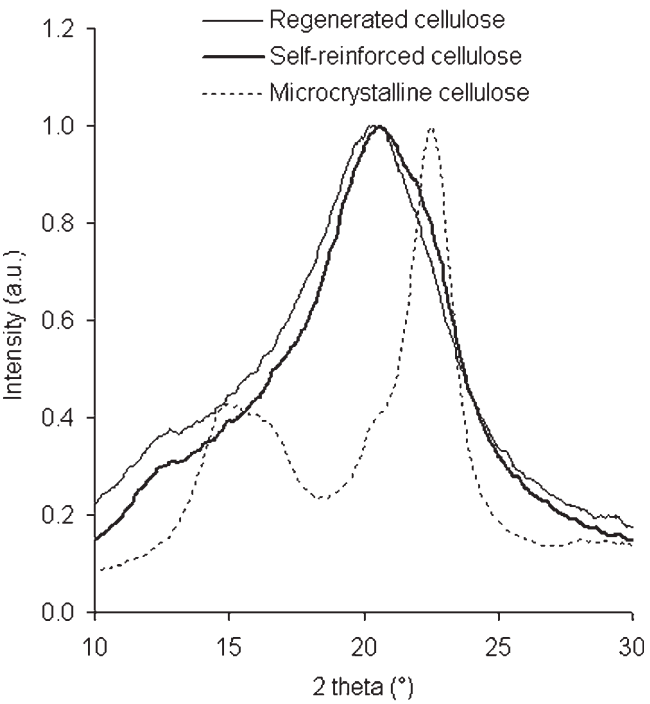

Figure 2 X-ray diffractograms of regenerated cellulose, microcrystalline cellulose (MCC), and a self-reinforced cellulose film containing cellulose I and cellulose II.

TABLE I
Summary of the Properties of Self-Reinforced Cellulose Films with Different Draw Ratio D_R

D_R	Δn	f_c	x_c (%)	E (GPa)	σ_f (MPa)	ε_f (%)
1	–	0.00	45.6	9.9	202	16.1
1.1	0.0078	0.07	45.2	14.6	252	9.1
1.25	0.0132	0.14	45.3	21.1	332	6.0
1.5	0.0325	0.29	45.6	33.5	428	2.3

Note: Δn – birefringence, f_c – crystalline orientation parameter, x_c – degree of crystallinity, E – modulus of elasticity, σ_f – tensile strength, ε_f – elongation at break.

which should facilitate drawing. Because of adsorption of water the cellulose film thickness increased by 35% from an initial dry thickness of 0.2 mm. This is significantly less than the thickness of 4 mm, which the films had immediately after coagulation before drying. This irreversible reduction of thickness indicates that the structure of self-reinforced films is changed and consolidated to a great extent during drying, a process termed hornification well known for cellulose fibers.[24]

The results of structural characterization by WAXS and birefringence measurements, and mechanical characterization by tensile testing are summarized in Table I. As seen in WAXS 2D detector images presented in Figure 3, drawing resulted in preferred

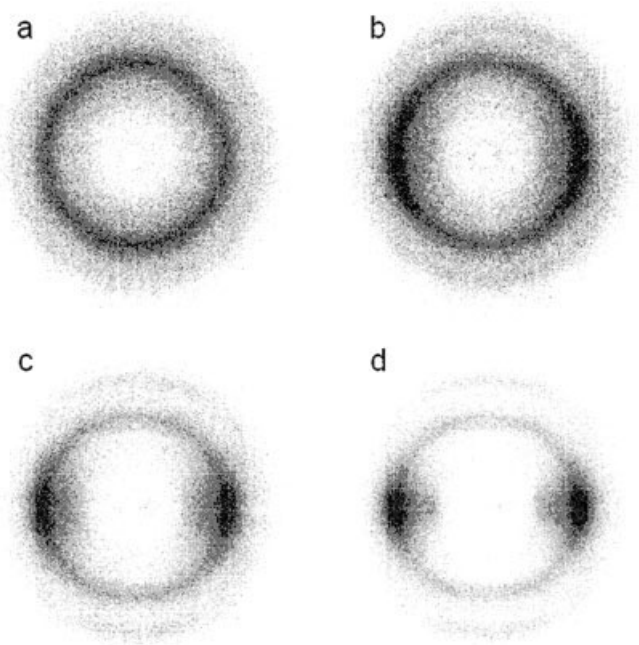

Figure 3 Wide angle x-ray scattering 2D detector images of an undrawn self-reinforced cellulose film with random orientation (a) and films with a draw ratio of 1.1 (b), 1.25 (c), and 1.5 (d). The integrated intensity distribution of the most intense reflection (combined cellulose I (200) and cellulose II (110/020) Debey-Scherrer ring) normal to the c crystallographic axis was evaluated for the determination of the orientation factor f_c.

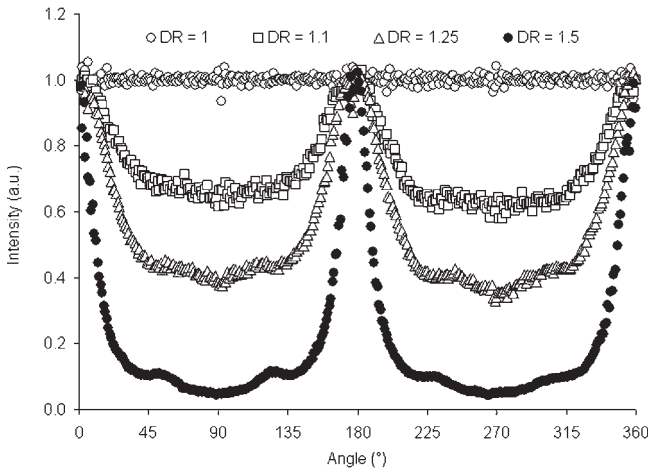

Figure 4 Integrated intensity distribution (combined cellulose II (110/020) and cellulose I 200 reflection) derived from WAXS data of an undrawn cellulose film and from films drawn to increasing draw ratio D_R.

orientation of the cellulose nanocrystallites in the self-reinforced films. The most intense reflection (combined cellulose I (200) and cellulose II (110/020) Debey-Scherrer ring) shows an isotropic intensity distribution in unstretched films (Fig. 4). Upon drawing, clear intensity maxima develop, indicating increasing preferred orientation of the *c* crystallographic axis of cellulose crystallites parallel to the direction of draw (Fig. 4). The crystalline orientation parameter f_c calculated from the integrated intensity distribution of WAXS 2D detector images increased linearly with increasing draw ratio (Fig. 5). This observation agrees well with *in situ* stretching experiments performed with dry self-reinforced cellulose films prepared according to the same procedure as described in the present study,[25] where a linear relationship was also observed between the applied tensile strain and the orientation of cellulose crystallites (f_c). Birefringence measurements performed on the cellulose films confirmed the WAXS results. The birefringence, like the crystalline orientation parameter, f_c, is proportional to the average degree of orientation of both the crystalline and amorphous phases, and showed a linear increase with increasing draw ratio (Table I, Fig. 5). Due to uncertainties regarding the correct value of $\Delta n_{\max}$ for cellulose,[22,26] the Herman's orientation factor was not calculated in the present study. Regarding crystalline orientation, a maximum f_c of 0.29 was achieved at a draw ratio of 1.5 (Table I). In comparison to regenerated cellulose fibers, where f_c in the order of 0.8 to > 0.9 is typical,[27] the maximum f_c of drawn self-reinforced cellulose films is rather modest. However, it has to be considered that in the case of regenerated cellulose fibers drawing takes place before or during coagulation in the spinning bath,[15] when the cellulose macromolecules are more mobile, whereas the films presented in this study were drawn with an already consolidated structure. Molecular modeling of strained amorphous cellulose[28] showed that yielding under strain occurs due to the disruption of intermolecular hydrogen bonds. New hydrogen bonds are formed in extension but only 1/3 of these are broken during recovery from strain. These newly formed hydrogen bonds were found to hold the cellulose chain segments in the new position,[28] thus resulting in poor deformation recovery, as shown also experimentally in cyclic loading-unloading of regenerated cellulose fibers.[27,29] The method of swelling cellulose in water, with subsequent drawing and drying in drawn state, thus profits from the rupture and reforming of hydrogen bonds in cellulose facilitated by adsorption of water. Desorption of water during drying reduces chain mobility and therefore the structure is arrested in a state of preferred orientation. Togawa and Kondo[30] reported on the drawing of never-dried regenerated cellulose films. This was also considered as a possible way of drawing in the present study but failed due to the fragility of self-reinforced cellulose in never-dried state, which is apparently more pronounced than for the pure regenerated cellulose used by Togawa and Kondo.[30] In addition to an increasing degree of orientation of the crystallographic *c* axis of cellulose parallel to the applied strain, no structural changes were discernible from WAXS (Table I). In particular, there was no change in the crystallinity of the cellulose films due to drawing (Table I), as is observed in the drawing of thermoplastic polymers like poly(ethylene terephthalate).[17] This observation agrees well with results obtained by drawing of highly amorphous never-dried cellulose films,[30] where no significant change in crystallinity was measured either. Togawa and Kondo[30] propose that cellulose chains can not change

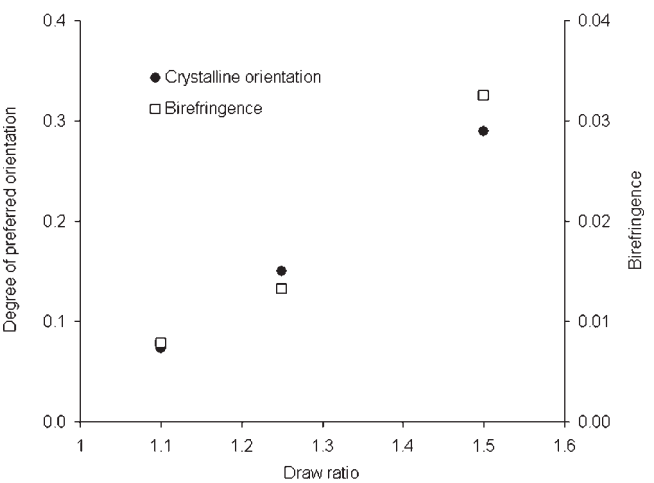

Figure 5 Relationship between draw ratio (D_R) and the crystalline orientation factor (f_c) and the overall orientation expressed by the sample birefringence (Δn), respectively.

their state from folded to fibrillar under strain due to the presence of intermolecular hydrogen bonding.

Tensile testing of drawn self-reinforced cellulose films shows the effect of increasing degree of preferred orientation on mechanical properties (Figs. 6 and 7). With increasing draw ratio, the tensile strength and the modulus of elasticity of self-reinforced cellulose films increase significantly in the direction of draw, while the elongation at break decreases in turn (Table I). On the other hand, mechanical properties transverse to the direction of draw undergo a significant decrease, with minimum values of 4.4 GPa for the modulus of elasticity and 95 MPa for tensile strength at a draw ratio of 1.5. Improved mechanical properties due to drawing (Table I) agree very well with the properties of regenerated cellulose fibers produced with different draw ratio. Similar to our results obtained with self-reinforced cellulose films, increasing draw results in higher orientation, higher tensile strength and modulus of elasticity, and reduced elongation at break.[22] Also in regenerated cellulose fibers, the relationship between draw ratio and elastic modulus and tensile strength, respectively, is linear as found in our experiments (Fig. 7).

The excellent mechanical properties of self-reinforced cellulose films produced in this study present a significant improvement with regard to cellophane and melt-blown cellulose films.[15] Also in comparison to a unidirectional ramie fiber-reinforced all-cellulose composite introduced by Nishino et al.,[12] which achieved a tensile strength of 480 MPa and a modulus of elasticity of 15–20 GPa (estimated from Ref. 12, Fig. 4), self-reinforced films are competitive regarding strength and superior regarding stiffness. The stiffness of oriented self-reinforced cellulose films is also highly competitive with industrially produced regenerated cellulose staple fibers (lyocell), which show typical modulus of elasticity of 22 GPa in spite of showing much higher degree of orientation than

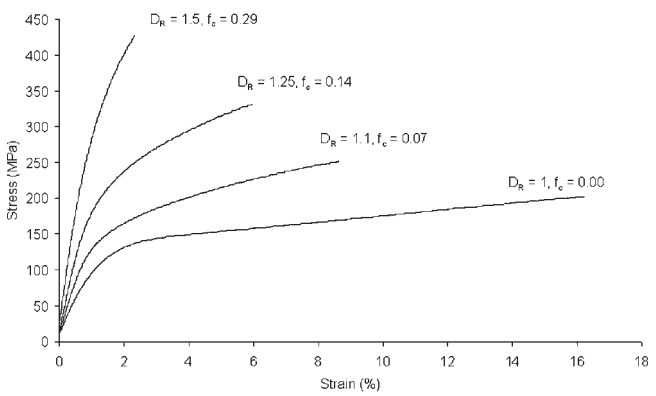

Figure 6 Representative stress-strain curves of self-reinforced cellulose films with different draw ratio (D_R) and orientation factor f_c.

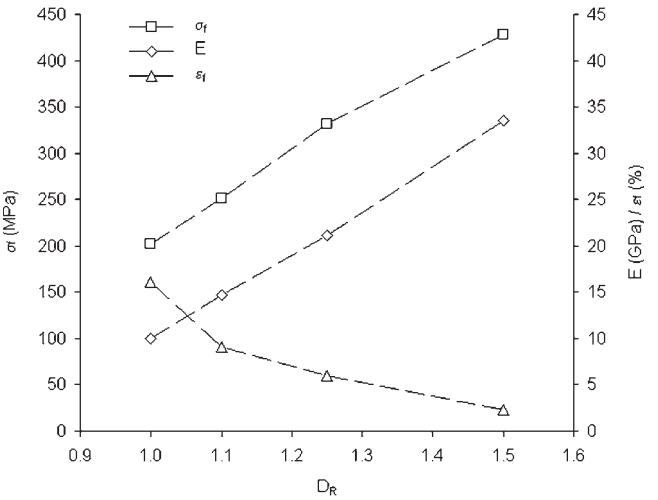

Figure 7 Relationship between the tensile strength (σ_f), the modulus of elasticity (E), the elongation at break (ε_f), and the draw ratio (D_R).

the films presented here.[27] This observation confirms the high impact of reinforcement of regenerated cellulose with high-modulus cellulose I particularly on stiffness. By comparison, current all-bio-based composites consisting of bio-based polymers such as poly lactic acid[6,7] and poly vinyl alcohol[31] reinforced by cellulosic fibers achieve only modest mechanical properties of 6 GPa for modulus of elasticity and 100 MPa for tensile strength.

CONCLUSIONS

From the results presented earlier, the following conclusions may be drawn:

- In spite of intense intermolecular hydrogen bonding, cellulose films can be drawn in water-swollen condition at ambient temperature up to a draw ratio of 1.5.
- In a linear relationship with draw ratio, drawing induces preferred orientation into the cellulose films, and the elastic modulus and tensile strength of the films increase proportionally.
- Because of their comparably high strength and stiffness, oriented self-reinforced films may present a potential route to produce all-bio-based materials, which are truly competitive with non-bio-based materials.

References

1. Gross, R. A.; Kalra, B. Science 2002, 297, 803.
2. Netravali, A. N.; Chabba, S. Mater Today 2003, 6, 22.
3. Pandey, J. K.; Kumar, A. P.; Misra, M.; Mohanty, A. K.; Drzal, L. T.; Singh, R. P. J Nanosci Nanotechnol 2005, 5, 497.
4. Ray, S. S.; Bousmina, M. Prog Mater Sci 2005, 50, 962.
5. Azizi Samir, A. S.; Alloin, F.; Dufresne, A. Biomacromolecules 2005, 6, 612.

6. Huda, M. S.; Mohanty, A. K.; Drzal, L. T.; Schut, E.; Misra, M. J Mater Sci 2005, 40, 4221.
7. Mathew, A. P.; Oksman, K.; Sain, M. J Appl Polym Sci 2005, 97, 2014.
8. Nishino, T.; Takano, K.; Nakamae, K. J Polym Sci Part B: Polym Phys 1995, 33, 1647.
9. Azizi Samir, A. S.; Alloin, F.; Paillet, M.; Dufresne, A. Macromolecules 2004, 37, 4313.
10. Nakagaito, A. N.; Iwamoto, S.; Yano, H. Appl Phys A 2005, 80, 93.
11. Nakagaito, A. N.; Yano, H. Appl Phys A 2005, 80, 155.
12. Nishino, T.; Matsuda, I.; Hirao, K. Macromolecules 2004, 37, 7683.
13. Gindl, W.; Keckes, J. Polymer 2005, 46, 10221.
14. Northolt, M. G.; den Decker, P.; Picken, S. J.; Baltussen, J. J. M.; Schlatmann, R. Adv Polym Sci 2005, 178, 1.
15. Fink, H. P.; Weigel, P.; Purz, H. J.; Ganster, J. Prog Polym Sci 2001, 26, 1473.
16. Allison, S. W.; Ward, I. M. Br J Appl Phys 1967, 18, 1151.
17. Ajji, A.; Cole, K. C.; Dumoulin, M. M.; Ward, I. M. Polym Eng Sci 1997, 37, 1801.
18. Carr, P. L.; Jakeways, R.; Klein, J. L.; Ward, I. M. J Polym Sci Part B: Polym Phys 1997, 35, 2465.
19. Matsuo, M.; Bin, Y.; Nakano, M. Polymer 2001, 42, 4687.
20. Hong, K.; Strobl, G. Macromolecules 2006, 39, 268.
21. Alexander, L. E. X-ray Diffraction Methods in Polymer Science; Wiley-Interscience: London, 1969.
22. Kong, K.; Eichhorn, S. J. Polymer 2005, 46, 6380.
23. Olsson, A.-M.; Salmen, L. Carbohydr Res 2004, 339, 813.
24. Crawshaw, J.; Cameron, R. E. Polymer 2000, 41, 4691.
25. Gindl, W.; Martinschitz, K. J.; Boesecke, P.; Keckes, J. Compos Sci Technol 2006, 66, 2639.
26. Lenz, J.; Schurz, J.; Wrentschur, E. Holzforschung 1994, 48, 72.
27. Gindl, W.; Keckes, J. Comp Sci Technol 2006, 66, 2049.
28. Chen, W.; Lickfield, G. C.; Yang, C. Q. Polymer 2004, 45, 1063.
29. Northolt, M. G.; Balthussen, J. J. M.; Schaffers-Korff, B. Polymer 1995, 36, 3485.
30. Togawa, E.; Kondo, T. J Polym Sci Part B: Polym Phys 1999, 37, 451.
31. Zimmermann, T.; Pöhler, E.; Geiger, T. Adv Eng Mater 2004, 6, 754.